Multi-Stage Control Strategy of IoT-Enabled Unmanned Vehicle Detection Systems

Hongyan Dui, Huanqi Zhang, Xinghui Dong, Shaomin Wu, and Yu Wang

***Abstract*— As the environment deteriorates, natural disasters occur more frequently and become more devastating to human beings and the environment. After a disaster, to quickly and optimally restore the damaged things, including physical systems (e.g., transport networks) and the environment, needs decision makers to own sufficient data/information. Unmanned vehicle detection systems (UVDS) are undoubtedly feasible tools in collecting such data in a harsh environment. The most important challenges in UVDS management are on modeling the UVDS data layer and multi-stage recovery strategies, which have received little research. To address such problems, this paper proposes a multi-stage control strategy for UVDS based on Internet of Things (IoT). The optimal decision is decided by utilizing four indicators: performance recovery efficiency, normal detection probability, operation cost, and economic benefit cost, respectively. The simulation results show that the proposed strategy improves the performance recovery efficiency by 12.1% and the normal detection probability by 3.9%, the operation cost declines by 58.4%, and the economic benefit cost by 75.9% compared with the general control strategy.**

***Index Terms*— Unmanned vehicle, control strategy, performance, Internet of Things, operational cost.**

I. Introduction

IN RECENT years, there has been an increasing number of natural disasters, which have caused an increasing death toll. For example, more than 250 earthquakes of magnitude M4.0 and above between 2021 and 2024, and 18 earthquakes of magnitude 5.0 and above occurred in 2023 alone occurred on the mainland. In the post-disaster rescue work, traditional manual detection strategies are slow and often fail to ensure rescue workers' safety. This leads to the possibility of missing the best rescue time and increasing the rescue burden. In harsh environment, unmanned vehicle detection systems (UVDS) can detect the designated area and collect data about the environments, which can accurately search the location of the people waiting to be rescued. The application of unmanned vehicles (UVs) greatly reduces the risk of rescue and increases the speed and success of rescue.

The development of Internet of Things (IoT) [1] technology has made unmanned devices more advantageous for data collection and regional environmental detection. Collecting data in harsh environments with the help of unmanned equipment is an efficient method. For example, Drăgulinescu et al. [2] developed a remote wide area network-based data collection framework, which can realize the auxiliary data collection of UVs in harsh environments. Vasudevan and Baskaran [3] developed an improved embedded system that allows UVs to better monitor water quality. Cai et al [4] proposed a lightweight water obstacle detection network architecture using IoT technology to ensure unmanned aerial vehicle (UAV) detection reliability in the ocean. Ke and Chen [5] used a particle swarm optimization algorithm to optimize an unmanned equipment detection system, so that the system can detect underwater targets efficiently and accurately. Yuan et al. [6] utilized unmanned equipment technology to detect and explore the marine environment. Li et al. [7] investigated UAVs for data collection in intelligent transportation systems and proposed a framework for controlling the flight speed of UAVs to improve the fairness of data collection. Bera et al. [8] proposed a scheme to optimize the trade-off between the number of IoT devices covered and the flight time of the UAV to better collect data for the cloth IoT devices.

However, UVDS may fail to perform detection missions, which greatly affects the speed and efficiency of rescue. Therefore, the challenge that properly commanding the UVDS to carry out the fault recovery under the condition of a certain cost is an intriguing research question. In addition, in the actual detection, the impact of the disaster shock on the signal transmission in the region is different because the level of the disaster shock is different at different locations. Thus, it is necessary to analyze the information propagation loss of UVDS. Conventional UVDS models seldom consider the information propagation process in the data layer, which motivates the research of the current paper.

A. Related Work

The operation of UVDS depends on the development of IoT. With the development of IoT technology, the intelligent technology of unmanned equipment has been well established. For example, Dui et al. [9] used advanced IoT technology to improve the intelligence level of the intelligent transportation

Received 21 May 2024; revised 23 November 2024; accepted 24 January 2025. This work was supported by the National Natural Science Foundation of China under Grant 72071182 and Grant 72301254. The Associate Editor for this article was K. Gao. *(Corresponding author: Hongyan Dui.)*

Hongyan Dui, Huanqi Zhang, and Yu Wang are with the School of Management, Zhengzhou University, Zhengzhou 450001, China (e-mail: duihongyan@zzu.edu.cn; zzuzhq@gs.zzu.edu.cn; ywang@zzu.edu.cn).

Xinghui Dong is with the College of Systems Engineering, National University of Defense Technology, Changsha 410073, China (e-mail: dxhnudt@163.com).

Shaomin Wu is with the Kent Business School, University of Kent, Canterbury, CT2 7FS Kent, U.K. (e-mail: S.M.Wu@kent.ac.uk).

Digital Object Identifier 10.1109/TITS.2025.3535737

system and provide an optimal control strategy for UVs. Yang et al. [10] constructed a UAV-assisted IoT resource allocation and control model by utilizing the IoT communication technology. Wu et al. [11] described how detection missions for underwater targets are realized by combining UAVs, UVs and the IoT. Fu et al. [12] investigated UAV-assisted IoT. A distributed user clustering algorithm was proposed to cluster IoT devices into multiple distributed user clusters.

The performance of a system is an important metric for evaluating the system. The performance can always reflect the state of the system, and several evaluation indicators can be evolved by analyzing the performance [13], [14] of the system, such as performance efficiency [15], [16], robustness [17], reliability [18], [19], and so on.

Performance recovery efficiency, as an important indicator of system, has received extensive attention from systems researchers for its unique properties. In the study of system performance efficiency. Dui et al. [20] proposed a new resilience model for systems facing competing risks to enhance the performance recovery efficiency of the system. Li et al. [21] optimized an urban rail transit system by considering the traffic congestion level over time to improve the overall performance efficiency of the system. Haghshenas et al. [22] proposed a cost-based optimization model after a dust storm. It improves the performance efficiency of the distribution system through maintenance crew routing and outage management. Chen et al. [23] explored the resilience of urban rail transit networks to enhance the performance recovery efficiency of the network with a fast method to restore connectivity of disrupted links. Li et al. [24] developed a fine-grained supply chain network model with product families and proposed a performance efficiency optimization strategy for the system based on the model.

To boost the normal detection probability of the system, Liu et al. [25] proposed a software belief reliability growth model based on uncertain differential equations, which improves the normal detection probability of software. Okyere et al. [26] investigated the ability of large-scale multi-input multi-output physical layer network coding to withstand jamming attacks in 6 GHz and millimeter-wave vehicular network systems, which greatly enhances the probability of proper network operation. Wang et al. [27] proposed a joint virtual network partitioning and hybrid backup scheme. This scheme can enhance the probability of working properly for virtualized network slicing.

Dui et al. [28] proposed a construction method of a dynamic maintenance strategy, which optimizes the cost for the process of producing data for the system. Levitin et al. [29] proposed an algorithm for evaluating the expected cost of a mission to obtain a mission allocation strategy that minimizes the cost of the mission. Dui et al. [30] proposed an IoT-based ground settlement-based risk warning and maintenance strategy optimization method. Wang et al. [31] developed a co-optimization model for the life cycle cost of BEB systems, which reduced the life cycle cost of overnight and opportunity fee systems by 7.77% and 6.64%, respectively. Lin and Tang [32] established a multi-objective public transport scheduling optimization model, which comprehensively considers the benefits of all parties and finally achieves the goal of optimizing the cost and time consumption of the system.

Through a comprehensive review of the available literature, we found that current research on UVDS has less analysis of the data layer. Even though some researchers have analyzed UVDS based on IoT, the constructed models lack data layer modeling. Meanwhile, the control process of UVDS is complex, but the current research lacks multi-stage control strategies for UVDS. Since performance efficiency can be a good measure of the system's ability to resist and recover from a blow, researchers mostly focus on the performance efficiency analysis of UVDS. This leads to an oversimplified study of UVDS and does not allow for a comprehensive assessment of UVDS. In post-disaster environment, the resources of UVDS are limited, which leads to the importance of resource optimization of UVDS. Currently, there is insufficient research on resource optimization in UVDS, and there is a lack of algorithms for optimizing the allocation of resources in UVDS. How to better control UVDS with limited resources is an urgent problem to be solved.

B. Contribution and Organization

From the above discussions, existing studies ignore the collaborative functionality of the physical and data layers in UVDS, but they rarely consider the multi-stage strategy of multiple indicators in UVDS and lack optimized resource allocation at limited cost especially in emergencies. In recent years, IoT has been increasingly used in UVDS. A challenge is to explore way to better utilize IoT technology to control and manage UVDS. The main contributions of this paper to the study of UVDS are as follows:

(1) Usually, the physical and data layers work in coordination with each other, and both layers are equally important in maintaining the normal operation of the system. On this basis, we propose the UVDS model under the synergistic effect of "physical" + "data". The failure mechanism, resource isomorphism and performance changes of the two layers are analyzed.

(2) For the control strategy of UVDS, which is often multi-staged, the indicators of each stage reflect the focus of the control decision. In this paper, we propose a multi-stage control strategy for UVDS. To improve the performance recovery efficiency of the system, a recovery sequence control decision of UV is proposed. To optimize the probability of normal operation of the system, a recovery mode decision for UV is proposed.

(3) Resource allocation optimization for UVDS is necessary in different scenarios. Especially in emergency situations where rescue resources are limited. To address this phenomenon, we give a method to calculate the cost of UVDS and propose an optimization algorithm to minimize the operational cost.

The rest of the paper as follows. In Section II, an IoT model based on UVDS is established. Section III analyzes the performance of the physical and data layers, as well as the failure mechanisms of the two layers in concert. In Section IV, a UVDS recovery sequence control decision based on performance recovery efficiency is proposed. In Section V,

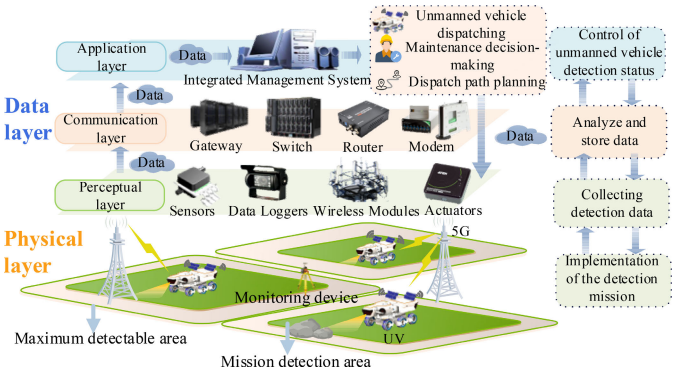

Fig. 1. IoT architecture for UVDS.

Fig. 2. Process of physical layer shocked.

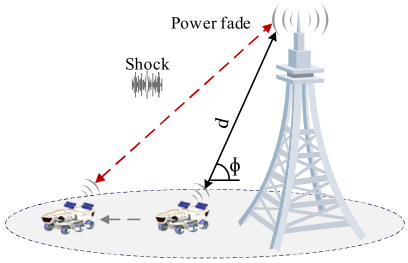

Fig. 3. Interference at the data layer.

a decision on the control method based on performance recovery time is proposed, considering different numbers of devices. A cost-based reordering method is proposed when multiple optimal recovery patterns and sequences exist. In Section VI, specific calculations are made using the 16 locations in Hebi that need to be tested as example. Section VII concludes this paper and proposes future work.

II. Modeling of UVDS Based On IoT Technology

A. Analysis of Multi-Tier Architecture for UVDS

UVDS is a complete control, actuation, and information transfer system with an IoT architecture divided into four layers, i.e., physical, perception, communication and application layers as shown in Fig. 1.

As illustrated in Fig. 1, a typical UVDS consists of four layers: physical, perceptual, communication, and application layers.

- The physical layer is the bottom layer of the UVDS, which is responsible for handling the acquisition of raw data between detection network devices.
- The perception layer is responsible for sensing various environmental parameters such as temperature, humidity, light intensity, motion status, to list a few. This layer collects environmental data after detecting a certain area, the middleware then converts the data into analog signals suitable for the transmission medium and converts the received analog signals back to digital data upon the reception.
- The communication layer is responsible for the transmission, routing and forwarding of data in the network. Various mechanisms and protocols in this layer, such as checksum, cyclic redundancy detection, retransmission mechanism, etc., can be used to detect and correct errors in the data to ensure the reliability and integrity of data transmission.
- The application layer is responsible for analyzing and making decisions on the detection data transmitted from the physical layer. Meanwhile, the application layer can monitor, deploy, manage the operation of the whole system and quickly restore the UVDS to the normal working state.

For the perception layer, communication layer and application layer, we focus on the changes in the performance of receiving, sending, and processing data among the layers. The data transmission among layers has the same transmission mechanism as the communication layer. To simplify the analysis among different layers, the three layers are referred to as data layers where needed.

B. Analysis of Failure Mechanisms in UVDS Multi-Tier Architecture

In the physical layer, after the detection equipment is subjected to natural aging and shocks, the detectable area will gradually become smaller. When the detectable area of the UV is smaller than its own detection mission area, it means that the UV cannot fulfill the detection mission. The failure is monitored by the application layer and the integrated management system will recover the UV. The process of the UVDS facing a shock is shown in Fig. 2.

As can be seen in Fig. 2, UV components can fail with the combination of external shocks and natural aging. Components such as tires, motors, sensors, and batteries are more susceptible.

Unlike the physical layer, when the data layer faces a shock, it mainly affects the received power of the receivers in the base station. When the received power is less than the decodable power, the performance of the data layer is 0. At the end of the impact, the normal state is automatically restored at the end of the shock, and the impact process is shown in Fig. 3.

The receiver is unable to decode the signal, resulting in signal interruption. The UV changes its position with respect to the base station during the detection process, and the path loss is greater when the object moves farther away from the base station, making it more susceptible to shocks. The initial frequencies of the transmitter and receiver are unaffected by the shock, but the signal interference from the shock increases the path loss during propagation, resulting in a decrease in the power of the signal as it propagates to the receiver.

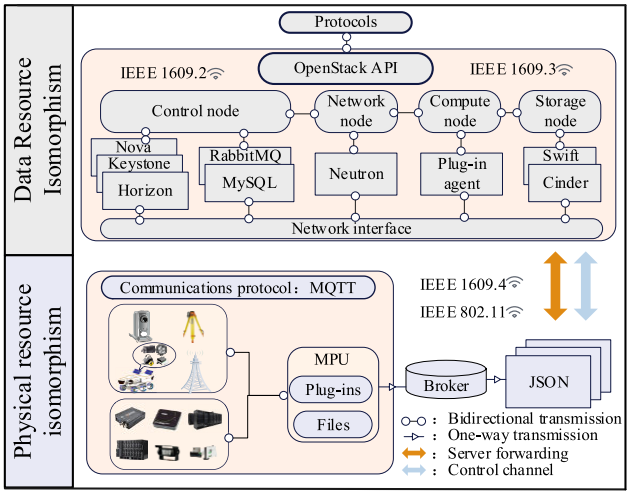

Fig. 4. Isomorphism of the layers of the UVDS.

C. Analyzing the Coupling Relationship of "Physical" + "Data" and Resource Isomorphism Processing of UVDS

In the detection network framework proposed in this paper, to ensure isomorphism of resources in the physical and data layers, there are relevant subsystems and protocols in UVDS that are responsible for the resource isomorphism of the physical and data layers to ensure compatibility among different devices, platforms, and protocols.

Ensuring interoperability and isomorphism between different physical layer resources is critical. This can be achieved by adopting a standardized communication protocol Message Queuing Telemetry Transport (MQTT) and data format Java Script Object Notation (JSON), which allows physical devices from different vendors and types to communicate and interact with each other.

For data layer resources, ensuring that they are isomorphic means that they can be managed and scheduled through a unified interface or protocol. This usually involves cloud computing platforms or virtualization management software that enables unified management and control of resources through OpenStack APIs [33] and management protocols.

The process of detecting the system to achieve isomorphism is shown in Fig. 4.

From Fig. 4, the device-level data will be transmitted to the OpenStack API protocol after receiving isomorphic processing. This not only contains the storage of the isomorphic device-level data but also allows isomorphic processing of data in the data layer. All the processed data will be fed back to the application layer so that the application layer can make faster and more accurate decisions.

III. Performance Analysis of UVDS Considering Physical and Data Layer Collaboration

A. Physical Layer Performance Analysis of UVDS

In UVs, the hardware of UV is so diverse and complex that it is difficult to quantify the impact of the hardware on the overall performance of UV. To simplify the complexity of the analysis, we do not perform component-level analysis. We use the UV as a research object for physical layer modeling and analysis. When the component level parts in the UVDS fail or age, the UVDS monitors the UV's performance degradation or is unable to fulfill its own detection task. Then, UVDS can transmit the data information back to the control center to make maintenance decisions.

The physical layer of the detection system is composed of clusters of UVs and related equipment. The performance of the UV is defined as the ratio of the detectable area to the initial detectable area at a certain point in time, as shown in (1).

$$P_n^c(t) = \frac{S_n(t)}{S_n(t_0)}, \tag{1}$$

where n is the number of UVs in the UVDS, $P_n^c(t)$ is the performance of the nth UV at time t, $S_n(t)$ is the detectable area of the nth UV at time t, and $S_n(t_0)$ is the detectable area of the nth UV at the initial moment

During a UV's detection mission, shocks may come from two sources: due to internal shocks such as natural aging or deterioration and due to external shocks, such as environmental impacts. The former occurs in the physical layer all the time, and the amount of change in performance is assumed to obey a linear relationship [34].

In the absence of external shocks, the natural aging of devices in the physical layer of the detection system conforms to an exponential decay model. [35]. We varied the decay model by taking the decay amount as the UV performance degradation amount to obtain the UV performance change under the influence of natural degradation only as shown in (2).

$$X_n^c(t) = \lambda_0(t - t_0)e^{\lambda_0(t-t_0)}, (t \geq t_0), \tag{2}$$

where $X_n^c(t)$ is the amount of performance degradation from t_0 to t, and λ_0 is the natural degradation parameter of UV.

The system is exposed to shock, which is essentially an acceleration of overall natural aging. We reflect this acceleration in the magnitude of the catastrophic shock, the duration of the shock, and the UV shock resistance value. The amount of degradation under the shocks suffered by UVs, $Y_n^c(t)$, is shown in (3).

$$\begin{cases} Y_n^c(t) = \lambda_i(t - t_a)\left(\dfrac{W_i(\Delta t)}{D_n(t)}\right)e^{\lambda_i(t-t_a)} \\ \Delta t = t - t_a, \end{cases} \tag{3}$$

where t_a is the shock starts time, λ_i is the shock degradation parameter of the ith time; $W_i(\Delta t)$ is the magnitude of the shock amplitude of the ith disaster during the period of Δt and $D_n(t)$ is the value of resistance to the shock of the nth UV at time t.

The resistance to shocks shows a decreasing trend as the number of shocks increases, and this decreasing trend we define obeys an exponential change based on the damage. The change of the UV's resistance to shocks is shown in (4).

$$D_n(t) = \left(1 - \beta_n^i m^{\beta_n^i(t-t_a)}\right)D_n(t_a), \tag{4}$$

where m is the total number of shocks to the UVDS, and β_n^i is the change parameter of the nth UV affected by the ith shock.

If the UV is restored to a new condition through a series of maintenance measures such as repair or replacement, the next

time the UV is impacted, it will have the same resistance as the first time it was impacted.

By combining (3) and (4), we can obtain the performance change of the UV as shown in (5).

$$Y_n^c(t) = \lambda_i (t - t_a)\, e^{\lambda_i (t - t_a)} \left(\frac{W_i(\Delta t)}{\left(1 - \beta_n^i m^{\beta_n^i (t - t_a)}\right) D_n(t_a)} \right). \tag{5}$$

When the detectable area of the UV is equal to the area for performing the mission, we define the performance of the UV currently as a threshold value. The performance threshold of the UV is shown in (6).

$$P_n^{limit} = \frac{S_n^{mission}}{S_n^{max}}, \tag{6}$$

where S_n^{max} is the maximum detectable area of the nth UV, $S_n^{mission}$ is the area of the nth UV for mission detection.

During the repair process, the performance recovery rate of UV is always changing. At the early stage of restoration, the UV is so damaged that it is difficult to repair and its performance enhancement rate is small. In the middle stage of restoration, the enhancement rate is faster. In the late stage of recovery, its recovery gradually reaches the optimal state, and the performance improvement rate decreases. As such, the performance recovery can be assumed to obey the logistic function [36], as shown in (7).

$$P_n^r(t) = \frac{1}{1 + e^{-\theta_n (t - t_n^a)}}, \tag{7}$$

where t_n^a is the time for the nth UV to start recovery, and θ_n is the recovery parameter of the nth UV. The value is derived by personnel based on a combination of several metrics, including the area of the UV's mission detection and recovery complexity. In this paper, the specific calculations are shown in (8).

$$\theta_n = \frac{S_n^{mission}}{\sum_{i=1}^{m} S_n^{mission}}. \tag{8}$$

The UV can be understood as a component in the detection system, and the change in the performance of each component has a different impact on the performance of the system. Thus, the recovery process of the UV for the UVDS is a process to enhance the performance of the system or to slow down the degradation of the UVDS performance.

B. Data Layer Performance Analysis of UVDS

It is difficult to analyze and quantify the changes in environmental conditions, sensor accuracy, and other factors that arise after a disaster. To explore the interference to the data layer, we performed a performance analysis of the data layer through the Free Space Path Loss Model (FSPL) [37] model. The impact generated after the disaster is measured in terms of the transmitted and received power of the signal. This analysis method covers many complex types of signal interference due to post-disaster environmental changes.

The performance degradation of the data layer is essentially signal attenuation between the signal transmitter and the signal receiver. The degree of attenuation is related to factors such as distance, frequency, and occurring power, so the signal attenuation during propagation conforms to FSPL. The FSPL is calculated as (9).

$$P_L(d) = 20 log_{10} \left(\frac{4\pi d f}{c} \right), \tag{9}$$

where $P_L(d)$ is the path loss in decibels (dB), d is the Euclidean distance between the transmitter and receiver (m), f is the frequency of the signal (HZ), and c is the speed of light $(3 \times 10^8 m/s)$.

Signal transmission in post-disaster environments is often affected by more obstacles, terrain changes, and multipath effects. The FSPL assumes that the signal propagates without complex path phenomena such as reflection, diffraction, or scattering, and is suitable for more open, obstacle-free environments. Therefore, the use of FSPL alone is inappropriate. For we transform the FSPL by introducing Rayleigh [38] distributed random variables, the transformation is as in (10).

$$P_L(d) = 20 log_{10} \left(\frac{4\pi d f}{c} \right) + 10 log_{10}(R), \tag{10}$$

where R is the random variable introduced by the Lowry distribution.

The R can be calculated as (11),

$$R = \sigma \cdot \sqrt[2]{-2 \ln U}, \quad U \in (0, 1], \tag{11}$$

where σ is the scale parameter of the Rayleigh distribution that controls the fading strength of the signal and U is a random variable obeying a uniform distribution.

The d can be calculated as (12).

$$d = \sqrt[2]{h^2 + s^2}, \tag{12}$$

where h is the height difference between the UV and the distance from the base station and s is the horizontal distance of UV from the base station.

We define G_n^s and G_n^r as the gain on the nth UV transmitter and base station receiver, respectively. This gain belongs to a directional antenna [39]. Combining the impact of the magnitude of the shock and combining it with (10) can be obtained as (13).

$$P_n^L(t) = 10 log_{10} \left(\left(\frac{4\pi d_n(t)\, f \sigma \sqrt[2]{-2 \ln U}}{G_n^s G_n^r c} \right)^2 \right) \frac{W_i(\Delta t)}{W}, \tag{13}$$

where W is the adjustment factor.

During the analysis, we choose the base station where the signal is transmitted as the base station with the closest Euclidean distance. This base station has a directional antenna, and the effect of signal fading from other base stations is not considered.

The UV will be displaced during the process of detection, and the movement will cause the distance d between the UV and the base station to change, and the nth UV's moving distance is shown in (14).

$$\Delta d_n = v_n \cdot cos \Phi_n \cdot \Delta t, \tag{14}$$

where Φ_n is the elevation angle formed by the initial position of the nth UV moving with the base station transmitting point, and v_n is the detection speed of the nth UV.

The phase change affected by the distance change is shown in (15).

$$\Delta\phi_n = \frac{2\pi v_n c}{f} \cdot cos\Phi_n \cdot \Delta t. \tag{15}$$

We analyzed the speed threshold of the UV and combined with (14), and (15), we can derive the doppler frequency [40] as (16).

$$f_{n,D}^{limit} = \frac{v_n c}{f} \cdot cos\Phi_n. \tag{16}$$

The application layer can assess the detection status of a UV by counting the Doppler shift $f_{n,D}^{limit}$ of a certain UV to determine whether the UV can complete the detection mission within the specified time.

We define the power of the transmitter as PO_n^s and the power of the receiver as PO_n^r, and the minimum decodable power as $PO_n^{r,min}$, then

$$P_n^{max}(t) = PO_n^s(t) - PO_n^{r,min}(t). \tag{17}$$

The performance of data propagation is defined as whether the receiver can decode properly. The data propagation performance is 0 if the path loss is too large, greater than the loss threshold $P_n^{max}(t)$, so that the receiver receives too little power to decode correctly. The UV data layer performance is calculated as (18).

$$P_n^d(t) = \begin{cases} 1, & \left(P_n^L(t) < P_n^{max}(t)\right) \\ 0, & \left(P_n^L(t) \geq P_n^{max}(t)\right) \end{cases} \tag{18}$$

IV. Recovery Sequence Control Decision for UVDS Based on Performance Recovery Efficiency

The data layer of UVDS does not act directly on the performance of the UV, and its signal reception state determines the state of UVDS. Therefore, the performance of UVDS can be calculated as (19).

$$P(t) = \frac{\sum_{n=1}^{m} P_n^d(t) \cdot P_n^c(t)}{m}, \tag{19}$$

where m denotes the number of UVs in the UVDS.

UVDS is a detection network composed of multiple UVs, which collaborate with each other to accomplish the detection missions in the area. The detection process will inevitably face failure conditions.

The performance recovery efficiency of UVDS is closely related to the change in system performance, and it reflects the performance expressiveness of the system during the recovery phase. A system with a high-performance recovery efficiency usually means that the UVDS can recover from shocks faster and detect missions faster, has higher performance, and overall performance. The performance recovery efficiency of UVDS is calculated as (20).

$$PE(t) = \frac{\int_{t_c^a}^{t_c^b} P(t)dt}{\int_{t_c^a}^{t_c^b} P\left(t_c^a\right)dt}, \tag{20}$$

where $PE(t)$ is the performance recovery efficiency of the system at t. t_c^a is the moment when UVDS starts to recover, and t_c^b is the moment when UVDS recovery ends.

To ensure that the UVDS accomplishes the mission within the specified time, the performance of the UV should be restored as soon as possible. How to optimize the performance recovery efficiency of the UVDS is the research focus of this section. Therefore, a sequential control decision based on performance recovery efficiency is proposed.

The impact of shocks on the performance is constant during the recovery process, so we do not consider shocks in the calculation of the recovery process. We assume that UV and UV are independent of each other and there is no dependency. That is, there is no synergy between UVs and UVs to perform tasks. The recovery rate of UVs depends mainly on the recovery parameter θ_n. We define that the nth UV starts the recovery at t_n^a, and finishes the recovery at t_n^b. The recovery rate indicates the amount of performance recovery per unit time, so the recovery rate for the nth UV is shown in (21).

$$I_n^r = \frac{\int_{t_n^a}^{t_n^b} P(t) - P\left(t_n^a\right) dt}{t_n^b - t_n^a}, \tag{21}$$

where I_n^r is the recovery rate of the nth UV.

According to (19), the amount of cumulative UV recovery is dispersed equally among all the UV in UVDS. Its rate of change is unaffected, so the recovery rate equation can be calculated from the UV recovery function alone, as shown in (22).

$$\begin{aligned} I_n^r &= \frac{\int_{t_n^a}^{t_n^b} [\left(\frac{1}{1+e^{-\theta_n(t-t_n^a)}} - \frac{1}{2}\right)]dt}{t_n^b - t_n^a} \\ &= \frac{\frac{1}{\theta_n}\ln\left(1+e^{\theta_n\left(t_n^b - t_n^a\right)}\right) - \frac{1}{\theta_n}\ln 2 - \frac{1}{2}\left(t_n^b - t_n^a\right)}{t_n^b - t_n^a}. \end{aligned} \tag{22}$$

Because $t_n^b - t_n^a > 0$, we analyze the monotonicity of (22) without considering the denominator. We let $\left(t_n^b - t_n^a\right) = \gamma, (\gamma > 0)$, $f(\theta_n) = \frac{1}{\theta_n}\ln\left(1+e^{\theta_n\gamma}\right) - \frac{1}{\theta_n}\ln 2 - \frac{1}{2}\gamma, m = e^{\theta_n\gamma}$. From (8), it follows that $0 < \theta_n < 1$, then $\theta_n = \frac{\ln m}{\gamma}, (2 < m)$.

Integrating over $f(\theta_n)$ we obtain (23).

$$f'(\theta_n) = \frac{\theta_n m\gamma + (1+m)\ln 2 - \ln(1+m)(1+m)}{\theta_n^2(1+m)} \tag{23}$$

Because $f'(\theta_n) > 0$, (23) is an increasing function.

The larger the θ_n of a UV, the faster its recovery rate is. To explore the recovery order of multiple UVs, based on the principle of maximizing the performance recovery efficiency, we need to find the ordering that can make the system obtain the maximum performance recovery efficiency.

Theorem 1: Prioritizing the recovery of UVs with larger recovery parameter, the higher the performance recovery efficiency of UVDS.

Proof of **Theorem 1**: Regardless of which recovery order is followed for recovery, all UVs will eventually return to their normal state and the total time spent on repairs will be the same. This results in the same performance at the beginning of the recovery and the same performance at the end of the UVDS for each strategy. So, we can set the performance at

initial recovery to 0. We assume that there are n UVs in the UVDS that are damaged at the same time. The recovery rates are sorted as follows: $I_1^r > I_2^r > I_3^r \ldots > I_n^r$, the repair time is $t_1^r, t_2^r, t_3^r \ldots t_n^r$.

To analyze the performance efficiency of UVDS, according to (20), we find that the denominator of (20) does not change, so we ignore the denominator and only calculate the numerator. After the above treatment, the recovery rate of UV can be expressed as: $I_n^r = \frac{\int_{t_n^a}^{t_n^b} P(t)dt}{t_n^r}$.

Then the performance efficiency of UVDS with UV recovery in the order of UV1→UV2→UV3→…→UVn recovery can be calculated as: $PE(\sum_{i=1}^{n} t_n^r) = I_1^r \cdot \sum_{i=1}^{n} t_n^r + I_2^r \cdot \sum_{i=2}^{n} t_n^r + \ldots + I_n^r \cdot t_n^r$. As can be seen from the above formula, the different order in which UVs are restored will result in different cumulative effects of their own. When the UV with a larger recovery rate is prioritized for recovery, its time during normal operation is longer, which allows the UVDS to obtain more cumulative performance. Therefore, the scheme of prioritizing the recovery according to the UV with larger recovery rate can achieve the optimum performance efficiency of the UVDS.

It has been shown above that the larger the θ_n of the UV, the larger the response rate of the UV. Therefore, prioritizing the recovery of UVs with larger θ_n leads to the best performance efficiency of UVDS.

Therefore, according to the **Theorem 1**. We can obtain:

It can be clearly seen that prioritizing recovery by following UVs with larger recovery parameters maximizes the performance recovery efficiency of UVDS.

V. UVDS Recovery Mode Control Decision Based on Performance Recovery Time

A. UVDS Performance Recovery Time Analysis

The performance recovery time of the UVDS is an important indicator of the normal detection of the UVDS, the shorter the performance recovery time, the higher the revenue that the system can create, and the higher the probability that the UVDS can detect normally.

The normal probability of detection at the physical layer is equal to the ratio of its normal detection time to the total detection time, as shown in (24).

$$R_c(t) = Pr\left\{ \begin{array}{l} \left(P_1^c(t) \geq P_1^{limit}\right) \cap \left(P_2^c(t) \geq P_2^{limit}\right) \cap \ldots \\ \cap \left(P_n^c(t) \geq P_n^{limit}\right) | t \leq t_{max} \end{array} \right\} = \frac{t_c^{normal}}{t}, \tag{24}$$

where t_c^{normal} is the time that physical layer can be detected normally, $R_c(t)$ is the probability of normal detection in the physical layer at t, and t_{max} is the total time for the UV to perform the mission.

The probability that the data layer works properly is based on the ratio of the time that the receiver of the numbered layers can decode the information properly to the total time, and the expression of the probability that the data layer can work properly is shown in (25).

$$R_d(t) = Pr\left\{ \left(\prod_{n=1}^{m} P_n^d(t) = 1 \right) | t \leq t_{max} \right\} = \frac{t_d^{normal}}{t}, \tag{25}$$

where $R_d(t)$ is the probability that the data layer can work properly at time t. t_d^{normal} is the time t at which the receiver at the data layer can decode normally.

Previously, we explored the synergistic analysis of the physical and data layers of the UVDS, so the normal detection probability of the UVDS can be calculated as (26).

$$R(t) = R_c(t) \cdot R_d(t) \tag{26}$$

The normal detection probability of the UVDS is the probability that the system is in a normal operating state. The higher the normal detection probability of the UVDS the longer it can be in normal operation during the same operating time, and the higher the revenue that can be generated by the UVDS.

According to (26) for calculating the normal detection probability of the UVDS, we find that to improve the normal detection probability of the UVDS, we need to minimize the repair time of the data layer and the recovery time of the UVs.

1) Performance Recovery Time Analysis for the Physical Layer: There are two ways of recovery for each vehicle: scheduling and repairing. Therefore, the calculation of the recovery time of the UVDS needs to be divided into two categories: schedule and repair.

Recovery time analysis for vehicle scheduling requires the calculation of the distance from the vehicle to be scheduled for the vehicle to be recovered. The distance is computed by the Floyd shortest path algorithm. Utilizing the algorithm requires the construction of a detection network and the matrix in the detection network is denoted by $Z(\tau, \alpha_{ij})$. Where τ is the number of all nodes in the matrix, usually the locations of UVs and maintenance squads and α_{ij} is the edges connecting all nodes to nodes in the detection network, which represents the recovery path. The states of any two of its nodes are represented by the criticality matrix, as shown in (27).

$$Z = \left[\alpha_{ij}\right]_{\tau \times \tau} = \begin{bmatrix} \alpha_{1,1} & \alpha_{1,2} & \ldots & \alpha_{1,\tau-1} & \alpha_{1,\tau} \\ \alpha_{2,1} & \alpha_{2,2} & \ldots & \alpha_{2,\tau-1} & \alpha_{2,\tau} \\ \vdots & \vdots & \ddots & \vdots & \vdots \\ \alpha_{\tau-1,1} & \alpha_{\tau-1,2} & \cdots & \alpha_{\tau-1,\tau-1} & \alpha_{\tau-1,\tau} \\ \alpha_{\tau,1} & \alpha_{\tau,2} & \cdots & \alpha_{\tau,\tau-1} & \alpha_{\tau,\tau} \end{bmatrix}. \tag{27}$$

For nodes that are not directly connected, we denote the distance between two points as $S_{ij} = inf$. The distance between neighboring nodes, it can be calculated based on the coordinates between the points in the matrix.

We can calculate the scheduling distance based on the Floyd shortest path algorithm, which is combined with the UV's scheduling speed to compute the scheduling time (i.e., the UV's performance recovery time). t_n^D represents the scheduling time of the Dth vehicle to the faulty vehicle n.

The recovery time analysis for vehicle repair requires calculating the distance between the vehicle to be repaired and

the repair squad and the time for the repair squad to repair. Similarly, the time consumed to reach the location to be repaired t_n^R can be calculated.

The repair time is related to the performance state that the UV is in. When the UV is subjected to a more severe level of shock, the more the UV's performance degrades and the longer it takes to repair. Based on (7), the recovery amount function of physical layer performance is used to calculate the repair time, which is shown in (28).

$$t_n^r = -\frac{1}{\theta_n} \cdot \ln \frac{1 - P_n^c\left(t_n^a\right)}{P_n^c\left(t_n^a\right)}, \tag{28}$$

where t_n^r is the repair time of the nth UV.

Therefore, the recovery time of the UV that is selected to be recovered by way of repair is $t_n^R + t_n^r$.

2) Performance Recovery Time Analysis for the Data Layer: We define that the recovery time of the data layer is related to the power received by the data layer, the lower the received power, the stronger the interference of the shock on the information propagation of the data layer is represented. This means that a stronger upgrading strategy is needed for the data layer to obtain a greater value of shock resistance. Thus, consuming more recovery time, the recovery time of the data layer is computed as shown in (29).

$$t_n^{d,repair} = \frac{PO_n^{r,min} - PO_n^r}{h}, \tag{29}$$

where h is the amount of power increase in the receiver between units.

B. Recovery Mode Control Decisions for A Single UV

When one UV is in the pending recovery state, the failure time is divided into recovery preparation time and recovery time, and the two recovery methods are analyzed separately as follows:

Decision 1: Scheduling

When using the scheduling scheme for recovery, we should first consider two conditions:

Condition 1: It is necessary to satisfy the UV that has completed its own detection mission normally before the failure of that UV, assuming that there are D vehicles to be scheduled and x vehicles with failures, which can be expressed as (30).

$$t_D^{finish} \le t_n^a, \tag{30}$$

where t_D^{finish} is the moment for the Dth vehicle to complete its own detection mission.

Condition 2: Whether the vehicle to be scheduled can take over the faulty UV to complete the remaining detection missions.

We can find out the scheduling distance from all the pending scheduling UVs to the faulty UV n. By comparing the paths of all the pending scheduling UVs, the shortest scheduling path is denoted as s_n^{min}, and the corresponding scheduling UV is D, the shortest scheduling recovery time that can be derived is shown in (31).

$$t_n^{min} = \frac{s_n^{min}}{v_D}, \tag{31}$$

where v_D is the traveling speed of the Dth UV.

The detection speed if the UV is in a normal state throughout is shown in (32).

$$v_n^{detect} = \frac{S_n^{mission}}{t_n^{detect}}, \tag{32}$$

where v_n^{detect} is the detectable area per unit of time.

However, the UV is unable to repair the detection speed normally after taking a shock. But in the process of waiting for scheduling, the UV is still detecting, and the detection area in the waiting process is shown in (33).

$$S_n^{wait}\left(t_n^a + t_n^{min}\right) = \frac{\int_{t_n^a}^{t_n^a + t_n^{min}} P_n^c(t)\,dt}{\int_{t_n^a}^{t_n^a + t_n^{min}} P_n^{limit}(t)\,dt} v_n^{detect} \cdot t_n^{min}, \tag{33}$$

where S_n^{wait} is the detection area of the pending UV to be restored while awaiting the dispatch process.

Then the detection area to be accomplished by the faulty UV is shown in (34).

$$S_n^{remain} = S_n^{mission} - S_n^{wait} - v_n^{detect} \cdot t_n^a, \tag{34}$$

where S_n^{remain} is the remaining detectable area of the faulty UV.

The detectable area of the vehicle to be scheduled can be calculated based on its own time to complete the detection mission, as shown in (35).

$$S_D\left(t_D^{finish}\right) = P_D^c\left(t_D^{finish}\right) \cdot S_D^{max}. \tag{35}$$

The scheduled UV must ensure that it has completed its own detection mission and can complete the remaining detection area of the malfunctioning UV.

Decision 2: Repair

To calculate the failure time of UVs when choosing a repair, we need to first calculate the repair arrival time t_n^R. The repair time t_n^r of the UV is calculated according to (28). Then the recovery time of the repair scheme is $t_n^R + t_n^r$.

Combining the two recovery schemes for a single faulty UV, when there exists $(t_D^{finish} \le t_n^a) \cap S_D\left(t_D^{finish}\right) > S_n^{remain}) \cap (t_n^{min} < t_n^R + t_n^r)$ we categorize this class of UVs to **Decision 1**, otherwise to **Decision 2**.

C. Multi-UV Recovery Approach Control Decision

It is often the case that multiple devices fail simultaneously after a shock to the UVDS. Based on this, a recovery sequencing of failed devices based on the recovery rate is proposed. When there are multiple UV failures, the best recovery method can be selected with limited recovery resources to maximize the uptime of the system for detection.

We are given that there are z (z is a positive integer) repair squads that can repair x malfunctioning UVs at the same time. Assuming that each vehicle is denoted as w_x, and the recovery ordering based on the recovery rate is $w_1, w_2 \ldots w_{x-1}, w_x$.

It can be divided into two cases:

When $z \ge x$, it indicates that all vehicles can be repaired at the same time, and the repair of $w_1, w_2 \ldots w_{x-1}, w_x$ can be

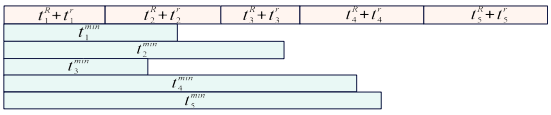

Fig. 5. Initial Gantt chart.

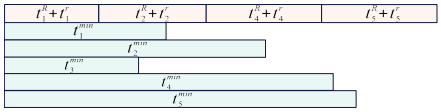

Fig. 6. Gantt chart after the first change.

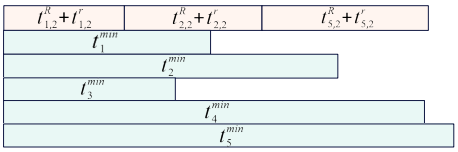

Fig. 7. Final Gantt chart.

regarded as a comparison of the simultaneous recovery scheme for each component and recovery at the same time.

When $z < x$, it indicates that the repair resources are limited and the recovery needs to start from the first ranked UV. By comparing the cumulative repair time and scheduling time, the vehicle recovery method is determined.

Assuming the arrangement according to the recovery rate is $w_1, w_2 \ldots w_{x-1}, w_x$. The cumulative repair time is the sum of the repair time of the previous x UVs, which is compared with the recovery time of the scheduling scheme, and the shorter recovery time is selected for recovery. If $(\sum_{y=1}^{x}(t_y^R + t_y^r) \geq t_y^{min})$, the scheduling scheme is selected to recover the UV. Otherwise, the repair scheme is selected to recover it.

It is important to note that when a vehicle chooses the scheduling option for recovery, the cumulative recovery time for subsequent UVs does not include the UVs that chose the scheduling option.

We take the number of repair squads as 1 and the number of UVs to be recovered as 5. A case is analyzed here:

(1) Suppose the UVs have the same recovery rate, assuming that the obtained recovery order is 1→2→(3,4)→5, in which UVs No. 3 and No. 4 have the same recovery rate. The treatment is that the full-arrangement computation of all the recovery scenarios can make the total recovery time T reach the shortest recovery order. The calculation of the total recovery time is not a simple summation calculation, the failures of different UVs will have different degrees of impact on the system, so the calculation of the total recovery time needs to be calculated in accordance with the recovery rate as the weighting of the weighted approach. The calculation is shown in (36).

$$T = \sum_{y=1}^{x} \frac{x \cdot \theta_y}{\sum_{y=1}^{x} \theta_y} \left(t_y^R + t_y^r\right). \tag{36}$$

The recovery is carried out in the order of 1→2→3→4→5. The recovery time of the UVs is represented by a Gantt chart, as shown in Fig. 5.

In Fig. 5, the repair time of the UV is shown in orange and the shortest scheduling time of the UV is shown in green. The recovery scenario of UV 1, which has a higher recovery rate, is smaller than the scheduling scenario, so UV1 chooses repair for recovery. The scheduling time of UV2 is greater than the cumulative time of repair for UV2, so the UV2 chooses the repair option for recovery. The scheduled time of UV3 is shorter, so 3 chooses the schedule option for recovery. We need to recalculate the recovery time of UVs 4 and 5 and the Gantt chart changes as shown in Fig. 6.

The cumulative repair time of UV4 is $\sum_{y=1}^{2}(t_y^R + t_y^r) + (t_4^R + t_4^r)$, which is still less than the time consumed by its scheduling scheme, and UV4 chooses to repair and recover. Similarly, UV5 chooses the scheduling scheme for recovery.

The total recovery time is

$$\begin{aligned} T = {} & \frac{4\theta_1}{\theta_1+\theta_2+\theta_4+\theta_5}\left(t_1^R + t_1^r\right) + \frac{4\theta_2}{\theta_1+\theta_2+\theta_4+\theta_5} \\ & \left(t_2^R + t_2^r\right) \\ & + \frac{4\theta_4}{\theta_1+\theta_2+\theta_4+\theta_5}(t_4^R + t_4^r) \\ & + \frac{4\theta_5}{\theta_1+\theta_2+\theta_4+\theta_5}(t_5^R + t_5^r). \end{aligned}$$

Similarly, the recovery proceeds in the order 1→2→4→3→5. The final Gantt chart is shown in Fig. 7.

The final total recovery time is $T = \frac{3\theta_1}{\theta_1+\theta_2+\theta_5}(t_{1,2}^R + t_{1,2}^r) + \frac{3\theta_2}{\theta_1+\theta_2+\theta_5}(t_{2,2}^R + t_{2,2}^r) + \frac{3\theta_5}{\theta_1+\theta_2+\theta_5}(t_{5,2}^R + t_{5,2}^r)$.

By comparing the total recovery time of the two different sequences, we find that following the sequence 1 → 2 → 4 → 3 → 5 clearly results in the shortest total recovery time, which can maximize the probability of normal detection of UVDS.

Special Situation: When there are multiple strategy approaches with the same total recovery time, we introduce two measures of operational cost and economic benefit cost.

In UVDS, operational cost and economic benefit cost are two key evaluation metrics that reflect the inputs and benefits of the system in terms of operations and economic benefit, respectively.

With limited funds, the lower the operating cost of UVDS, the less resource wastage can be reduced. The energy of UV can be optimized, and the system can achieve longer operation and high efficiency with limited resources.

The lower economic benefit cost indicates that the UVDS can better balance the cost input and optimize the economic benefit cost of the system. The remaining resource can be fully and reasonably utilized for the system's technology development and updating to enhance detection capability and adaptability.

The operational cost of UVDS includes several aspects. For example, power consumption costs, periodic maintenance costs, software update and maintenance costs, infrastructure costs, etc. These costs are too diverse to be analyzed in their entirety. Instead of the operational cost of UVDS, we have selected four major categories of representative costs to be analyzed. The operational cost of the UVDS can be divided into four aspects: loss cost, recovery cost, replacement cost and schedule cost.

1) Loss Cost: The system generates a certain amount of profit per unit of time in normal detection. The loss cost due to shocks is related to the length of time the system is in a low performance state. The lower the performance state in which the system operates, the higher the operational loss cost incurred, and the loss cost is calculated as shown in (37).

$$C_1 = z \cdot \left(1 - \frac{\int_0^{t_{max}} P(t)dt}{\int_0^{t_{max}} P(t_0)dt}\right), \tag{37}$$

where z is the benefits generated by the UVDS in the ideal state.

2) Recovery Cost: The physical layer recovery cost consists of the recovery preparation cost and the recovery cost. The recovery preparation cost is proportional to the time to arrive at the recovery location with a coefficient of K. The recovery cost is proportional to the recovery time with a coefficient of k. Therefore, the recovery cost of the physical layer, C_2^c is computed as shown in (38).

$$C_2^c = \sum_{x=1}^{w} K \cdot t_x^R + \sum_{x=1}^{w} k \cdot t_x^r, \tag{38}$$

where w is the number of cars that need to be repaired.

The data layer recovery cost is the cost incurred during the repair process. ϑ is the cost incurred per unit time of recovery. The recovery cost C_2^d of the data layer is shown in (39).

$$C_2^d = \vartheta \cdot t_d^{fault}. \tag{39}$$

The recovery cost of UVDS is $C_2 = C_2^c + C_2^d$.

3) Replacement Cost: Assume that from the beginning to the end of the operation, the component replacement cost of the xth UV is ε_x, which is replaced q_1 times. The physical layer replacement cost, C_3^c, can be calculated as (40).

$$C_3^c = \sum_{x=1}^{q_1} \varepsilon_x. \tag{40}$$

Similarly, the data layer replacement cost is φ_x each time the data layer is replaced q_2 times. The data layer replacement cost C_3^d can be calculated as (41).

$$C_3^d = \sum_{x=1}^{q_2} \varphi_x. \tag{41}$$

The replacement cost of the system is $C_3 = C_3^c + C_3^d$.

4) Schedule Cost: The unit distance cost incurred by UV is denoted by ∂. The calculation of the cost incurred by the call is shown in (42).

$$C_4 = \partial \cdot \sum_{x=1}^{\delta} s_x^{min}, \tag{42}$$

where δ is the total number of times that the UV is scheduled.

The operational cost of UVDS can be calculated as $C = C_1 + C_2 + C_3 + C_4$. The cost incurred during the operation of UVDS in $[0, t_{max}]$ cannot exceed the maximum budget value C_{bd}.

The cost optimization algorithm aims to develop an objective planning model for the operational cost and economic benefit costing of the recovery process of complex systems. Since the recovery of UVDS is considered, the cost of operational losses is the same for each scenario at that stage, and the cost of the data layer is also the same. Therefore, only the repair cost, replacement cost, or scheduling cost of the physical layer is considered in the algorithm.

We compare the Øth recovery scenario with the same total recovery time. The number of UVs selected for scheduling recovery under the Øth scenario is G. The set of scheduling times in the order of recovery of the identified UVs $A = [t_a^{\emptyset}, t_b^{\emptyset}, \ldots, t_d^{\emptyset}, t_e^{\emptyset}]$. The number of UVs selected for repair recovery is U. The set of repairing ready time in the order is $B = [t_{H,1}^{\emptyset}, \ldots, t_{Q,1}^{\emptyset}]$. The corresponding recovery time set is $C = [t_{H,2}^{\emptyset}, \ldots, t_{Q,2}^{\emptyset}]$. The maximum value of the time in the three sets is $t_e^{\emptyset}$, which corresponds to replacement cost $D = [\varepsilon_H, \ldots, \varepsilon_Q]$. The corresponding restoration cost under the Øth scenario is denoted by $C_c^{\emptyset}$. The economic benefit cost is $C_e^{\emptyset}$ and the optimal economic benefit cost is C_e^{min}. The number of programs with the same operational costs is . The optimal ordering is set A_c^{min}. The algorithm as follows:

Algorithm 1 Cost Optimization Algorithm

Input: $t_e^{\emptyset}$, K, k, ∂, $A = [t_a^{\emptyset}, t_b^{\emptyset}, \ldots, t_d^{\emptyset}, t_e^{\emptyset}]$, $B = [t_{H,1}^{\emptyset}, t_{I,1}^{\emptyset}, \ldots, t_{P,1}^{\emptyset}, t_{Q,1}^{\emptyset}]$, $C = [t_{H,2}^{\emptyset}, t_{I,2}^{\emptyset}, \ldots, t_{P,2}^{\emptyset}, t_{Q,2}^{\emptyset}]$, $D = [\varepsilon_H, \varepsilon_I, \ldots, \varepsilon_P, \varepsilon_Q]$

Output: C_e^{min}, A_c^{min}

Initialize: $C_c^{\emptyset} = 0$, $C_e^{\emptyset} = 0$

1. The set that arranges the elements of set A in order from smallest to largest is stored as $A_1 = [t_b^{\emptyset}, t_a^{\emptyset}, \ldots, t_e^{\emptyset}, t_d^{\emptyset}]$
2. Write the corresponding scheduling cost variation function under the Øth scenario:

$for\ i = 1 : length(t)$
$if\ t(i) > 0 \&\& t(i) <= t_b^{\emptyset}$
$C_A(i) = G \cdot t(i) \cdot \partial;$
$elseif\ t(i) > t_b^{\emptyset} \&\& t(i) <= t_a^{\emptyset} + t_b^{\emptyset}$
$C_A(i) = C\left(find\left(t = t_b^{\emptyset}\right)\right) + (G-1) \cdot \left(t(i) - t_b^{\emptyset}\right) \cdot \partial;$
end

3. Corresponding recovery cost change function under scenario Ø

$for\ i = 1 : length(t)$
$if\ t(i) > 0 \&\& t(i) <= t_{H,1}^{\emptyset}$
$C_B(i) = K \cdot t(i);$
$elseif\ t(i) > t_{H,1}^{\emptyset} \&\& t(i) <= t_{H,1}^{\emptyset} + t_{H,2}^{\emptyset}$
$C_B(i) = C\left(find\left(t = t_{H,1}^{\emptyset}\right)\right) + k \cdot t + \varepsilon_H;$
end

$$C_c^{\emptyset} = C\left(t_e^{\emptyset}\right) = C_A\left(t_e^{\emptyset}\right) + C_B(t_e^{\emptyset})$$

4. Identify the option with the lowest operational cost.
$If\ ב = 1$
This decision is A_c^{min}
$elseif\ ב > 1$
5. Calculate economic benefit cost $C_e^{\emptyset} = \int_0^{t_e^{\emptyset}} C(t)dt$, The least economic benefit cost is A_c^{min}.

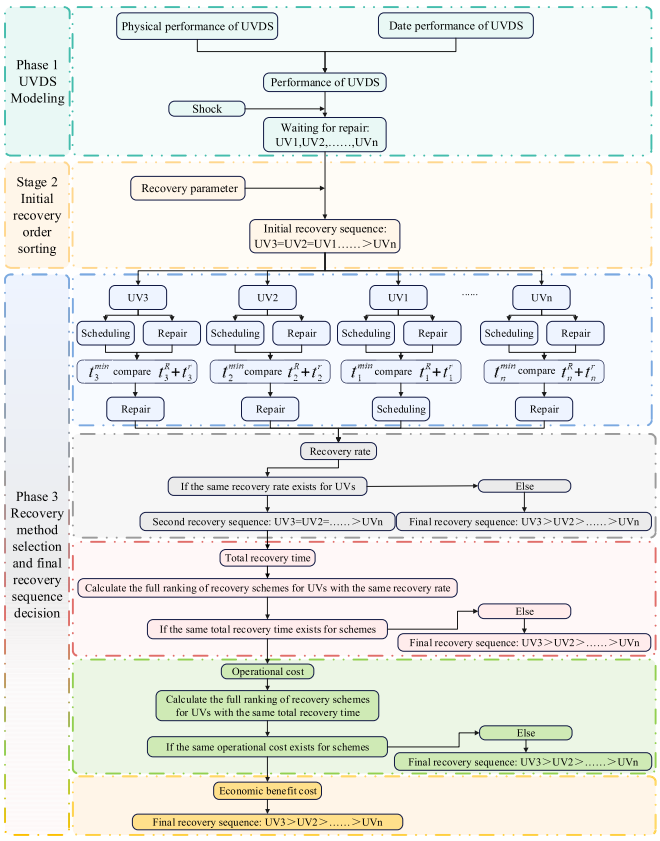

Fig. 8. Multi-stage control strategy flowchart.

To better show the process of the multi-stage control strategy proposed in this paper. We have drawn a flowchart for the multi-stage control strategy, as shown in Fig. 8.

VI. Experimental Validation

Terrain detection can help city planners better understand the topographic features of the area where the city is located, including information on terrain height, water distribution, land use conditions, and so on. Through exploration, data such as digital elevation models and digital terrain models can be obtained, which can be used to carry out urban planning, transportation planning, water resource management, natural disaster risk assessment and other work. Therefore, terrain exploration is an essential step before building a sponge city, which can provide important basic data and support for urban planning and construction.

Hebi located in the northern part of Henan Province, China, and its water environment problems are particularly prominent. Statistically, the average multi-year precipitation is 664.9 millimeters, and the per capita water resource is only 205 cubic meters, which is about 1/2 of the per capita water resource in the province and 1/10 of the per capita water resource in the country. To solve such problems, Hebi was identified as one of the first sponge city construction pilots in China in April 2015, and the ground condition covering an area of 29.8 square kilometers was subjected to surveying and data collection. The exploration mission ended in May 2019, during which several UVs failed, seriously affecting the progress of the sponge city mission. The specific application area of the control management proposed in this paper is shown in Fig. 9.

Fig. 9. Geographical location of the study area in Hebi.

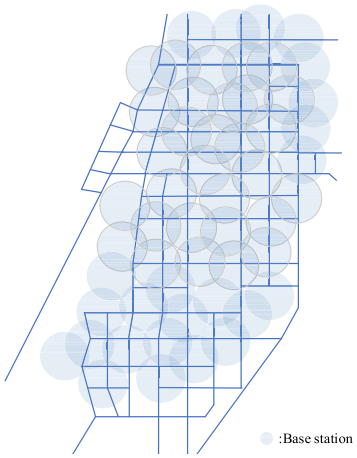

Fig. 10. Distribution of base stations in Hebi.

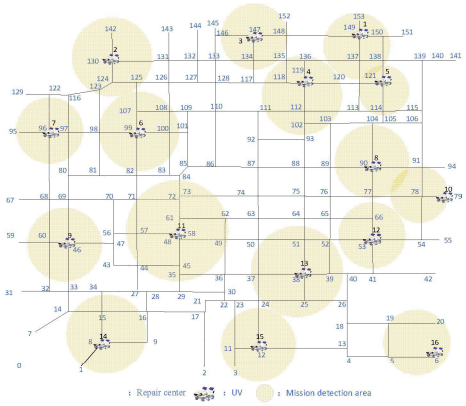

Fig. 11. Detection network.

The base station location[1] and distribution are shown in Fig. 10.

The base station is full coverage with a coverage density of $100m^2/per$. The total detection time of $100h$. The detection network mapping[2] for its main detection areas is shown in Fig. 11.

[1]https://www.189.cn/wap/telefivemap/telefivemap_hot.html?undefined
[2]https://www.henan.gov.cn/2018/12-10/725472.html

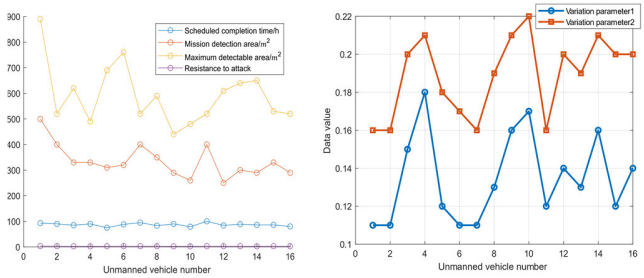

Fig. 12. Statistical chart of UV data values.

There are 16 UVs and 1 repair station in UVDS. The data detected by the UV is sent to the nearest base station based on the destination address. The data of each UV such as the completion of detection time, the maximum detectable area, and the mission detection area are shown in Fig. 12.

We define that the frequency of external shocks on the system obeys a Poisson distribution of 5×10^{-3}, and the average number of shocks received in $100h$ is two. The shocks occur at moments $t = 30$, $t = 80$. The strength of the disaster shocks $W_1 = 3.5$, $W_2 = 3.2$, adjustment factor $W = 5$. The duration of the two shocks is $9h$ and $10h$. The natural degradation rate parameter $\lambda_0 = 1 \times 10^{-4}$ for the UV, the parameter $\lambda_1 = 1 \times 10^{-2}$ for the first shock of the disaster on the physical layer, and $\lambda_2 = 1 \times 10^{-2}$ for the second shock of the disaster.

The performance changes during the completion of the detection mission of the UV1 are first calculated:

The UV1 is analyzed and there is no disaster shock before $30h$. The damage to the UV1 is caused by natural aging. According to (2) of the natural aging performance change function, calculate $P_1^c(30) = 0.997$, $P_1^c(30) = 0.997$.

According to (5) of the shock function, the performance of the UVs at the end of the shock is calculated as $P_1^c(39) = 0.885$.

UV1 is only affected by natural degradation from $t = 39$h to $t = 80$h. The system performance is calculated as $P_1^c(80) = 0.880$. UV1 can still detect normally.

The second shock comes, we need to calculate the anti-shock value of UV1 after experiencing the first shock. According to (4), we can calculate $D_1(80) = 3.06$, $W_{k2} = 3.2 > D(80)$, so the second shock will cause performance loss to UV1. Calculate the change the performance of UV1 after the second shock, $P_1^c(90) = 0.656 > 0.56$, which indicates that after the second shock, the performance of UV1 will change. We calculate the performance change $P_1^c(93) = 0.656$ for the whole probing mission. It means that UV1 completes the detection mission normally without any faults, and there is no recovery process for UV1.

To explore the recovery process, we continue to analyze UV2:

The change in performance of UV2 is the same as 1 until $30h$, then $P_2^c(30) = 0.997$, $P_2^c(39) = 0.864$ and $P_2^c(80) = 0.860$. We find that at $t = 85$. UV2 reaches a performance threshold. Without knowing the performance of the other UVs, we are unable to analyze the scheduling plan for the first phase.

TABLE I
SCHEDULE DISTANCE

UV	3	5	8	10	12	16	S_n^m/km^2
2	3.79	6.95	8.39	9.01	10.1	12.7	3.79
4	2.48	1.78	3.57	5.08	5.30	8.74	1.78
7	6.22	8.08	8.35	10.6	9.95	13.6	6.22
9	8.31	9.97	8.78	9.70	7.39	10.7	7.39
11	5.53	7.19	6.00	6.92	4.61	8.53	4.61

We perform the same analysis on the remaining 14 UVs and get: when $t = 85h$, the UVs 2, 4, 7, 9, and 11 are faulty. We recover the faulty UVs according to the proposed control management method.

The problem is a multi-device failure type. First, the order of the faulty UVs is sorted. The recovery rate of the UVs to be recovered is $\theta_2 = 5.53 \times 10^{-2}$, $\theta_4 = 4.57 \times 10^{-2}$, $\theta_7 = 5.53 \times 10^{-2}$, $\theta_9 = 4.68 \times 10^{-2}$, $\theta_{11} = 5.53 \times 10^{-2}$. According to the nature of the recovery rate, it can be seen that when $t = 85h$, the recovery order is (2, 7, 11)→9→4. Based on the recovery of multi-device faults with the same recovery rate, we compare the total downtime of all the schemes.

The first analysis follows the recovery sequence of 2→7→11→9→4.

To analyze the first stage, according to the above analysis, it is known that UVs 3, 5, 8, 10, 12, and 16 all have completed their own missions. We can obtain the maximum detectable area of each of the six vehicles after completing their missions: $S_3^{max}(85) = 440m^2$, $S_5^{max}(75) = 590m^2$, $S_8^{max}(83) = 480m^2$, $S_{10}^{max}(79) = 390m^2$, $S_{12}^{max}(84) = 460m^2$, $S_{16}^{max}(80) = 440m^2$. We compute the remaining detection area of the UV at the time of the fault. The UV fault occurs now when the probing task is about to be completed. A simple comparison shows that UVs 3, 5, 8, 10, 12, and 16 can satisfy the first and second conditions of the scheduling.

We analyze the dispatch time of the UV to be recovered. According to Floyd shortest path algorithm, and analyzing the scheduling time, the shortest distance (km) for the vehicle to be scheduled to reach the vehicle to be recovered is obtained, as shown in TABLE I.

Because the UVs is mainly dedicated to the detection mission, the UV is slower in the traveling process. We unify the speed of UV $v_m = 3.5km/h$, we can calculate the shortest call time of each faulty UV $t_2^3 = 1.08$h, $t_4^5 = 0.51$h, $t_7^3 = 1.78$h, $t_9^{12} = 2.11$h, $t_{11}^{12} = 1.32$h.

The speed of the repairer is $v = 20km/h$, and we calculate the repair time required for the repairer to reach UV 2 from the repair center as $t_2^R = 0.32$h. The arrival time for the repair is calculated in the order of 2→7→11→9→4 as $t_7^R = 0.15$h, $t_{11}^R = 0.27$h, $t_9^R = 0.14$h, $t_4^R = 0.42$h. Subsequent repair times and repair methods may change because of the change in repair methods of the previous UVs. We first calculate the recovery of the first UV. When the repairer arrives at UV2, $P_2^c(85.32) = 0.762$. The repair time of UV2 the time is $t_2^r = 0.31$h. Compared with the scheduling method, the UV2 chooses the repair method for recovery. Calculate the repair time of UV7, and the $t_7^r = 0.33$h. By comparing with the accumulated time, UV7 chooses the repair method for recovery. In the same analysis, UV11 chooses recovery plan.

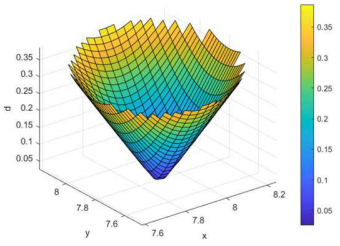

Fig. 13. Variation of d-value for UV1.

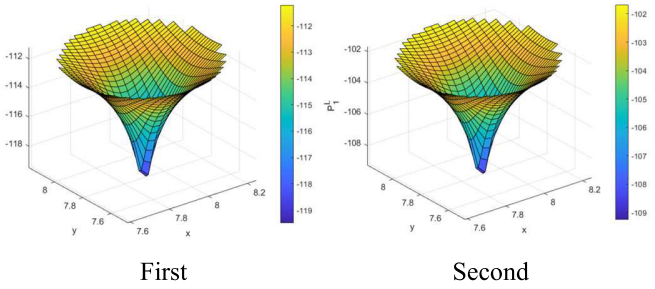

Fig. 14. Path loss of UV1 under two shocks.

UV9 chooses repair for recovery with repair time $t_9^r = 0.61$h. UV4 chooses restoration schedule. The total recovery time is calculated as $T_1 = 1.85$h according to (36).

Similarly, we analyze the recovery order according to 2→11→7→9→4, the total recovery time is $T_2 = 1.98$h.

Following the recovery order of 7→2→11→9→4, the total recovery time is $T_3 = 1.98$h.

Following the recovery order of 7→11→2→9→4, the total recovery time can be obtained as $T_4 = 1.98$h.

Following the recovery order of 11→2→7→9→4, the total recovery time can be obtained as $T_5 = 2.11$h.

Following the recovery order of 11→7→2→9→4, the total recovery time can be obtained as $T_6 = 1.77$h.

Following the recovery order of 11→7→2→9→4 can all lead to the shortest total recovery time of the system. This calculation example does not involve the case where the total recovery time is the same for multiple scenarios, so UVs 11, 7, and 9 choose the repair method for recovery, and the UVs 2, and 4 choose the scheduling method for repair.

The normal detection probability of the physical layer can be calculated according to (24), $R_c\,(100) = 0.982$.

The performance recovery efficiency and normal detection probability of the UVDS are calculated according to (20) and (26). We calculate operational cost and economic benefit cost using a cost optimization algorithm, and we can get $z = 5000$, $K = 10$, $k = 60$, $\varepsilon_{11} = 340$, $\varepsilon_2 = 160$, $\varepsilon_7 = 250$, $\varepsilon_9 = 330$, $\varepsilon_4 = 160$, $\tau = 300$.

The UVDS was in an open area at the time of this detection mission, so it could be analyzed using the FPLS model of (9). We unify the reception sensitivity of the 5G base station as $-120dBm$, the height $h = 30m$, and the transmitter power of the UV is $30dBm$. It can be calculated by (17) to get $P_L^{max}(t) = 150dBm$. By calculating the distance of UV1 from the base station in the detection mission, we can get the variation of distance d as shown in Fig. 13.

Based on the range of d values, the path loss under two impacts can be calculated, and the variation of loss values is shown in Fig. 14.

From Fig.14, the power of the signal of UV1 arriving at the base station under two shocks is always less than P_L^{max}(t). So, the data layer performance of UV1 is 1.

Similarly, analyzing the remaining 15 UVs, we found no data layer failures. Therefore, the performance of the data layer is 1. According to (25), the normal detection probability of the data layer $R_d\,(100) = 1$. The normal detection probability of the UVDS can be calculated according to (26), $R\,(100) = 0.982$. The data for all indicators of UVDS is shown in TABLE II.

TABLE II
THE VALUES FOR EACH INDICATOR

C.M.	R.S.	R.	S.	P.R.E.	N.D.P.	O.C.	C.E.B.
a	11→7→2 →9→4	11, 7,9	2,4	0.855	0.982	1128	1232

The C.M. stands for control management; R.S. for recovery sequence of UVs; R. for UVs selected for repair; s. for UVs selected for dispatch; P.R.E. for performance recovery efficiency; N.D.P. for normal detection probability; O.C. for operational cost, and C.E.B. for economic benefit cost.

To further demonstrate the effectiveness of the multi-stage control strategy proposed in this paper, we chose to compare two common recovery methods, namely, recovery according to the shortest traveling distance and recovery according to the length of repair time. The metrics of UVDS for the four strategies under the two restoration methods are calculated.

Based on the shortest distance recovery method, we find that the recovery order of 11→9→7→2→4 can minimize the distance of repair. The recovery order determined based on the recovery method of repair time is 2→11→7→4→9. Each repair order corresponds to the two types of strategy of using the repair method and scheduling method.

We analyze the performance variations of the to-be-recovered UVs and the UVDS. The changes in performance of all the UVs and the UVDS from $t = 80h$ to $t = 100h$, as in Fig. 15.

In Fig. 15, the blue line indicates the control strategy a, the red color indicates the control strategy b, the yellow color indicates the control strategy c, the purple color indicates the control strategy d, and the green color indicates the control strategy e. Among them, control strategies b, c, d and e are all common conventional control strategies. The control strategy a is the multi-stage control strategy proposed in paper, which allows the UV to recover at an earlier time.

Computing the performance recovery efficiency, the normal detection probability, the operational cost, and the economic benefit cost of the UVDS under the four types of recovery schemes are shown in TABLE III.

As can be seen from TABLE II and TABLE III, compared with the traditional control management method, the performance recovery efficiency is improved by 9.8%, 12.1%, 10.6%, and 10.9%, respectively. The probability of system detectability increased by 2.7%, 0.7%, 3.9%, and 1.0%,

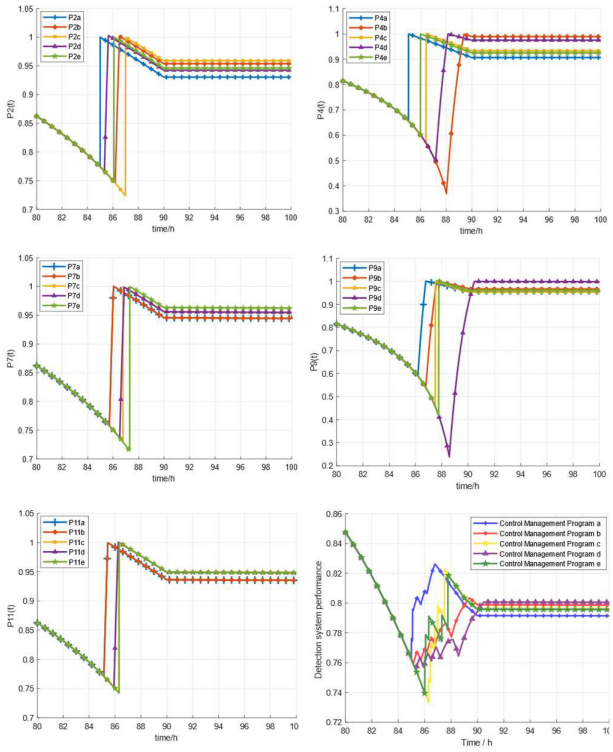

Fig. 15. Performance under five control strategies.

TABLE III
INDICATOR DATA UNDER FOUR-MANAGEMENT CONTROL

C.M.	R.S.	R.	S.	P.R.E.	N.D.P.	O.C.	C.E.B.
b	11→9→7 →2→4	11,9, 7,2,4		0.779	0.956	1442	4375
c	11→9→7 →2→4		11,9, 7,2,4	0.763	0.975	2712	4219
d	2→11→7 →4→9	2,11, 7,4,9		0.773	0.945	1488	5113
e	2→11→7 →4→9		2,11, 7,4,9	0.771	0.972	2550	4520

respectively. The operational cost is reduced by 21.8%, 58.4%, 22.1%, and 55.8%, respectively. The economic benefit cost is reduced by 71.8%, 70.8%, 75.9%, and 72.7%, respectively.

A comparison of the four indicators for the five strategies is shown in Fig. 16.

From the comparison of the five indicators in Fig. 16, it can be found that the UVDS control management proposed in this paper has significant advantages. Firstly, for the control management strategy of UVDS, the performance degradation trend can be calculated by sensing the magnitude of the environmental shocks through the sensors on the UV. The performance degradation curve can be plotted. Second, based on the performance recovery efficiency of the UVDS, the probability of the normal detection and operational cost and other indicators can help decision makers to judge the priority of UV recovery and recovery methods. Finally, with the help of IoT technology, the monitoring center can analyze the transmitted data in real time, and the managers can dispatch recovery personnel in an orderly manner to ensure that resources are effectively utilized and respond to pending repairs in a timely manner to minimize potential problems.

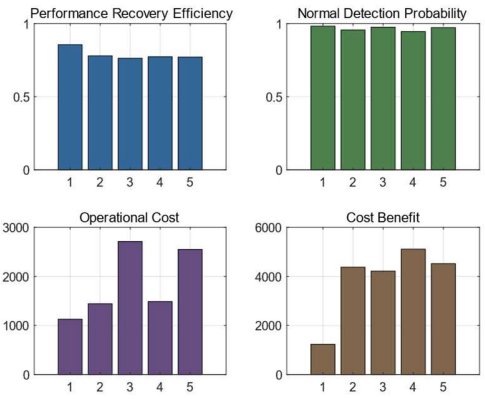

Fig. 16. Indicator values under the five strategies.

VII. CONCLUSION AND FUTURE WORK

This paper proposed a comprehensive modeling method of UVDS, which focused on the performance changes of the physical and data layers of UVDS under external shocks. In terms of the recovery strategy, a multi-stage control strategy was proposed. In the first stage, the performance recovery efficiency of the UVDS was analyzed and a decision was made on the recovery sequence of the UV. In the second stage, the recovery of UVs was decided based on the number of devices. A weight-based total recovery time calculation method was introduced to make the recovery mode decision based on the normal operation probability of UVDS. At the same time, considering the special case of the existence of multiple identical recovery strategies with the same probability of normal system detectability, we gave further control strategy based on the operating cost and the economic benefit cost. The results showed that to maximize the performance recovery efficiency and normal detectability probability of UVDS, the sequence and mode of faulty UV recovery needed to be considered to reduce the downtime of UV recovery.

In the future, the method of failure prediction can be integrated into the proposed recovery strategy, which provides a new idea for multi-stage control strategy. The UV and UV dependence studies were added to the multi-stage control strategy. Our future work focuses on:

(1) Autonomous Failure Prediction and Strategy Development: We aim to develop short-term performance change prediction methods based on the IoT technology to capture past inspection data or environmental data. The management gives instructions in advance to deploy the maintenance team in advance.
(2) Real-time data processing: we will develop simplified data processing channels for UVs to quickly convert monitoring data obtained from probes into actionable insights that can be used to adjust strategies in a timely manner.
(3) A study of the dependence between UV and UV: we will focus on the correlation between UV and UV for correlation modeling to enhance the applicability and comprehensiveness of multi-stage control strategies.

REFERENCES

[1] M. Adil, M. A. Jan, Y. Liu, H. Abulkasim, A. Farouk, and H. Song, "A systematic survey: Security threats to UAV-aided IoT applications, taxonomy, current challenges and requirements with future research directions," *IEEE Trans. Intell. Transp. Syst.*, vol. 24, no. 2, pp. 1437–1455, Feb. 2023, doi: 10.1109/TITS.2022.3220043.

[2] A.-M. Drăgulinescu, C. Zamfirescu, S. Halunga, I. Marcu, F. Y. Li, and O. A. Dobre, "Understanding LoRaWAN transmissions in harsh environments: A measurement-based campaign through unmanned aerial/surface vehicles," *IEEE Trans. Instrum. Meas.*, vol. 73, pp. 1–14, 2024, doi: 10.1109/TIM.2024.3351262.

[3] S. K. Vasudevan and B. Baskaran, "An improved real-time water quality monitoring embedded system with IoT on unmanned surface vehicle," *Ecological Informat.*, vol. 65, Nov. 2021, Art. no. 101421, doi: 10.1016/j.ecoinf.2021.101421.

[4] Q. Cai, Q. Wang, Y. Zhang, Z. He, and Y. Zhang, "LWDNet–A lightweight water-obstacles detection network for unmanned surface vehicles," *Robot. Auto. Syst.*, vol. 166, Aug. 2023, Art. no. 104453, doi: 10.1016/j.robot.2023.104453.

[5] C. Ke and H. Chen, "Cooperative path planning for air–sea heterogeneous unmanned vehicles using search-and-tracking mission," *Ocean Eng.*, vol. 262, Oct. 2022, Art. no. 112020, doi: 10.1016/j.oceaneng.2022.112020.

[6] S. Yuan et al., "Marine environmental monitoring with unmanned vehicle platforms: Present applications and future prospects," *Sci. Total Environ.*, vol. 858, Feb. 2023, Art. no. 159741, doi: 10.1016/j.scitotenv.2022.159741.

[7] X. Li, J. Tan, A. Liu, P. Vijayakumar, N. Kumar, and M. Alazab, "A novel UAV-enabled data collection scheme for intelligent transportation system through UAV speed control," *IEEE Trans. Intell. Transp. Syst.*, vol. 22, no. 4, pp. 2100–2110, Apr. 2021, doi: 10.1109/TITS.2020.3040557.

[8] A. Bera, S. Misra, C. Chatterjee, and S. Mao, "CEDAN: Cost-effective data aggregation for UAV-enabled IoT networks," *IEEE Trans. Mobile Comput.*, vol. 22, no. 9, pp. 5053–5063, Sep. 2023, doi: 10.1109/TMC.2022.3172444.

[9] H. Dui, S. Zhang, M. Liu, X. Dong, and G. Bai, "IoT-enabled real-time traffic monitoring and control management for intelligent transportation systems," *IEEE Internet Things J.*, vol. 11, no. 9, pp. 15842–15854, May 2024, doi: 10.1109/JIOT.2024.3351908.

[10] G. Yang and Y. Yao, "Resource allocation control of UAV-assisted IoT communication device," *IEEE Trans. Intell. Transp. Syst.*, vol. 24, no. 11, pp. 13341–13349, Nov. 2023, doi: 10.1109/TITS.2022.3219048.

[11] Y. Wu, K. H. Low, and C. Lv, "Cooperative path planning for heterogeneous unmanned vehicles in a search-and-track mission aiming at an underwater target," *IEEE Trans. Veh. Technol.*, vol. 69, no. 6, pp. 6782–6787, Jun. 2020, doi: 10.1109/TVT.2020.2991983.

[12] S. Fu, Y. Tang, N. Zhang, L. Zhao, S. Wu, and X. Jian, "Joint unmanned aerial vehicle (UAV) deployment and power control for Internet of Things networks," *IEEE Trans. Veh. Technol.*, vol. 69, no. 4, pp. 4367–4378, Apr. 2020, doi: 10.1109/TVT.2020.2975031.

[13] Y. Xu, Z. Long, Z. Zhao, M. Zhai, and Z. Wang, "Real-time stability performance monitoring and evaluation of Maglev trains' levitation system: A data-driven approach," *IEEE Trans. Intell. Transp. Syst.*, vol. 23, no. 3, pp. 1912–1923, Mar. 2022, doi: 10.1109/TITS.2020.3029905.

[14] C. Xu et al., "An efficient deployment scheme with network performance modeling for underwater wireless sensor networks," *IEEE Internet Things J.*, vol. 11, no. 5, pp. 8345–8359, Mar. 2024, doi: 10.1109/JIOT.2023.3318222.

[15] L. Liu et al., "Leveraging heterogeneous power for improving datacenter efficiency and resiliency," *IEEE Comput. Archit. Lett.*, vol. 14, no. 1, pp. 41–45, Jan. 2015, doi: 10.1109/LCA.2014.2363084.

[16] T. Wei, S. Liu, and X. Du, "Learning-based efficient sparse sensing and recovery for privacy-aware IoMT," *IEEE Internet Things J.*, vol. 9, no. 12, pp. 9948–9959, Jun. 2022, doi: 10.1109/JIOT.2022.3163593.

[17] K. Lee, S. E. Li, and D. Kum, "Synthesis of robust lane keeping systems: Impact of controller and design parameters on system performance," *IEEE Trans. Intell. Transp. Syst.*, vol. 20, no. 8, pp. 3129–3141, Aug. 2019, doi: 10.1109/TITS.2018.2873101.

[18] K. E. S. Desikan, V. J. Kotagi, and C. S. R. Murthy, "Decoding the interplay between latency, reliability, cost, and energy while provisioning resources in fog-computing-enabled IoT networks," *IEEE Internet Things J.*, vol. 10, no. 3, pp. 2404–2416, Feb. 2023, doi: 10.1109/JIOT.2022.3211872.

[19] B. Barabino, M. Di Francesco, and S. Mozzoni, "An offline framework for the diagnosis of time reliability by automatic vehicle location data," *IEEE Trans. Intell. Transp. Syst.*, vol. 18, no. 3, pp. 583–594, Mar. 2017, doi: 10.1109/TITS.2016.2581024.

[20] H. Dui, Y. Lu, and L. Chen, "Importance-based system cost management and failure risk analysis for different phases in life cycle," *Rel. Eng. Syst. Saf.*, vol. 242, Feb. 2024, Art. no. 109785, doi: 10.1016/j.ress.2023.109785.

[21] Z. Li, J. Yin, S. Chai, T. Tang, and L. Yang, "Optimization of system resilience in urban rail systems: Train rescheduling considering congestions of stations," *Comput. Ind. Eng.*, vol. 185, Nov. 2023, Art. no. 109657, doi: 10.1016/j.cie.2023.109657.

[22] M. Haghshenas, R.-A. Hooshmand, and M. Gholipour, "A novel cost-based optimization model for electric power distribution systems resilience improvement under dust storms," *Int. J. Crit. Infrastruct. Protection*, vol. 44, Mar. 2024, Art. no. 100659, doi: 10.1016/j.ijcip.2023.100659.

[23] J. Chen, J. Liu, B. Du, Q. Peng, and Y. Yin, "Resilience assessment of an urban rail transit network under short-term operational disturbances," *IEEE Trans. Intell. Transp. Syst.*, vol. 23, no. 12, pp. 24841–24853, Dec. 2022, doi: 10.1109/TITS.2022.3195937.

[24] W. Li, X. Song, K. Gong, and B. Sun, "A product family-based supply chain hypernetwork resilience optimization strategy," *Comput. Ind. Eng.*, vol. 187, Jan. 2024, Art. no. 109781, doi: 10.1016/j.cie.2023.109781.

[25] Z. Liu, S. Yang, M. Yang, and R. Kang, "Software belief reliability growth model based on uncertain differential equation," *IEEE Trans. Rel.*, vol. 71, no. 2, pp. 775–787, Jun. 2022, doi: 10.1109/TR.2022.3154770.

[26] B. Okyere, L. Musavian, B. Özbek, S. A. Busari, and J. Gonzalez, "The resilience of massive MIMO PNC to jamming attacks in vehicular networks," *IEEE Trans. Intell. Transp. Syst.*, vol. 22, no. 7, pp. 4110–4117, Jul. 2021, doi: 10.1109/TITS.2020.3016907.

[27] W. Wang, L. Tang, T. Liu, X. He, C. Liang, and Q. Chen, "Toward reliability-enhanced, delay-guaranteed dynamic network slicing: A multiagent DQN approach with an action space reduction strategy," *IEEE Internet Things J.*, vol. 11, no. 6, pp. 9282–9297, Jun. 2024, doi: 10.1109/JIOT.2023.3323817.

[28] H. Dui, X. Dong, and M. Liu, "A data-driven construction method of aggregated value chain in three phases for manufacturing enterprises," *Comput. Ind. Eng.*, vol. 189, Mar. 2024, Art. no. 109964, doi: 10.1016/j.cie.2024.109964.

[29] G. Levitin, L. Xing, and Y. Dai, "Optimal tasks assignment policy in multi-task multi-attempt missions," *Rel. Eng. Syst. Saf.*, vol. 243, Mar. 2024, Art. no. 109855, doi: 10.1016/j.ress.2023.109855.

[30] H. Dui, X. Dong, X. Wu, L. Chen, and G. Bai, "IoT-enabled risk warning and maintenance strategy optimization for tunnel-induced ground settlement," *IEEE Internet Things J.*, vol. 11, no. 13, pp. 22966–22981, Jul. 2024, doi: 10.1109/JIOT.2024.3377440.

[31] Y. Wang, C. Lu, J. Bi, Q. Sai, and X. Qu, "Lifecycle cost optimization for electric bus systems with different charging methods: Collaborative optimization of infrastructure procurement and fleet scheduling," *IEEE Trans. Intell. Transp. Syst.*, vol. 24, no. 3, pp. 2842–2861, Mar. 2023, doi: 10.1109/TITS.2022.3223028.

[32] H. Lin and C. Tang, "Analysis and optimization of urban public transport lines based on multiobjective adaptive particle swarm optimization," *IEEE Trans. Intell. Transp. Syst.*, vol. 23, no. 9, pp. 16786–16798, Sep. 2022, doi: 10.1109/TITS.2021.3086808.

[33] Z. Benomar et al., "A fog-based architecture for latency-sensitive monitoring applications in industrial Internet of Things," *IEEE Internet Things J.*, vol. 10, no. 3, pp. 1908–1918, Feb. 2023, doi: 10.1109/JIOT.2021.3138691.

[34] S. Hao, J. Yang, X. Ma, and Y. Zhao, "Reliability modeling for mutually dependent competing failure processes due to degradation and random shocks," *Appl. Math. Model.*, vol. 51, pp. 232–249, Nov. 2017, doi: 10.1016/j.apm.2017.06.014.

[35] Q. Feng et al., "Resilience measure and formation reconfiguration optimization for multi-UAV systems," *IEEE Internet Things J.*, vol. 11, no. 6, pp. 10616–10626, Mar. 2024, doi: 10.1109/JIOT.2023.3326552.

[36] T. Avinadav and T. Raz, "A new inverted U-shape hazard function," *IEEE Trans. Rel.*, vol. 57, no. 1, pp. 32–40, Mar. 2008, doi: 10.1109/TR.2007.909773.

[37] H. Fernández, L. Rubio, V. M. Rodrigo-Peñarrocha, and J. Reig, "Path loss characterization for vehicular communications at 700 MHz and 5.9 GHz under LOS and NLOS conditions," *IEEE Antennas Wireless Propag. Lett.*, vol. 13, pp. 931–934, 2014, doi: 10.1109/LAWP.2014.2322261.

[38] Y. Ai, M. Cheffena, A. Mathur, and H. Lei, "On physical layer security of double Rayleigh fading channels for vehicular communications," *IEEE Wireless Commun. Lett.*, vol. 7, no. 6, pp. 1038–1041, Dec. 2018, doi: 10.1109/LWC.2018.2852765.
[39] J. L. Volakis, *Antenna Engineering Handbook*. New York, NY, USA: McGraw-Hill, 2007.
[40] J.-G. Seo, I.-H. Lee, H. Jung, D. Benevides da Costa, and H. Shin, "Doppler characterization in LEO satellite-aided UAV swarm networks," *IEEE Wireless Commun. Lett.*, vol. 13, no. 4, pp. 1178–1182, Apr. 2024, doi: 10.1109/LWC.2024.3364172.

Hongyan Dui received the Ph.D. degree in management science and engineering from Northwestern Polytechnical University, China, in 2013.

He visited the Department of Systems Engineering and Engineering Management, City University of Hong Kong, many times as a Research Fellow, from 2014 to 2019. He is currently a Professor with the School of Management, Zhengzhou University, Zhengzhou, China. His proposed importance measure has been incorporated into the JMP software at SAS System, USA. He has published over 80 journal articles. His recent research interests include reliability and resilience modeling, analysis and optimization of complex systems and networks, wireless sensor networks, and the IoT systems and applications.

Huanqi Zhang is currently pursuing the Ph.D. degree with the School of Management, Zhengzhou University, Zhengzhou, China.

His research interests include reliability model, wireless sensor networks, and the IoT systems and applications.

Xinghui Dong is currently pursuing the Ph.D. degree with the College of Systems Engineering, National University of Defense Technology, Changsha, China.

His research interests include reliability models, wireless sensor networks, and the IoT systems and applications.

Shaomin Wu received the M.Sc. and Ph.D. degrees in applied statistics.

Before moving to the University of Kent, he was a Senior Lecturer in risk and decision analysis at Cranfield University. His research interests include recurrent event data analysis, machine learning, risk analysis, and security analysis. He is a member of the editorial boards of seven journals.

Yu Wang received the Ph.D. degree in management science and engineering from Tianjin University, China, in 2020.

He is currently an Assistant Professor with the School of Management, Zhengzhou University, Zhengzhou, China. His research interests include wireless sensor networks and the IoT systems.